ISSN: 2414-1895 DOI: 10.6919/ICJE.202301_9(1).0002

Finite Element Analysis of SRM Bonding Interface Structure under Vertical Storage

Kangjia Li[1, a], Hongfu Qiang[1], Zhejun Wang[1, b] and Zhaojun Zhu[2]

[1] Rocket Force University of Engineering, Xi'an 710025, China

[2] Zhengzhou University of Aeronautics, Zhengzhou 450015, China

[a] 1278671762@qq.com, [b] qinglongzaitian888@163.com

Abstract

During long-term vertical storage, SRM with high loading ratios and large diameters are more prone to long-term stress on the bonding interface due to propellant creep, resulting in degradation of the mechanical properties of the interface. In this paper, the mechanical response of the interface was obtained by carrying out simulation calculations of the whole SRM under vertical storage conditions. The study shows that the danger point of the bonding structure under vertical storage of SRM mainly exists at the root of the stress release of the insulation, which is subjected to the maximum stress, but the long-term load does not exceed 0.1 MPa, and the root of the stress release is subjected to multi-directional mixed stress.

Keywords

Vertical Storage; Bonding Interface; Finite Element; Stress State.

1. Introduction

With the diversification of military missions and changing warfare paradigms, silo launch has gradually become a new combat style for solid missiles. During the vertical storage of solid missiles in silos, the long-term gravitational force causes creep in the solid rocket motor (SRM) pillar, and the creep deformation of the pillar will damage the structure and performance of the charge bonding interface, thus affecting the structural integrity of the solid motor. Wang et al [1] showed that the creep damage of SRM pillar under long-term vertical storage is small, and the possibility of damage inside the pillar is small, so the focus should be on the failure and debonding of the bonding interface. As a typical failure site of the charge structure, the performance degradation and damage failure of the bonding interface directly affect the normal operation of the engine, and the application of a new generation of Nitrate Ester Plasticized Polyether (NEPE) high-energy solid propellant has also put forward higher requirements on the long-term mechanical performance of the bonding interface. Therefore, in order to accurately evaluate the mechanical properties of the SRM bonding interface with NEPE propellant as the pillar in long-term storage, this paper obtains the stress state of the interface structure of the whole SRM under vertical storage conditions through simulation analysis, and provides a reference and basis for experimental research according to the stress condition of the bonding interface.

Propellant self-weight is the biggest factor affecting the mechanical properties of the interface under vertical storage, which makes the interface under long-term stress. The propellants currently used in SRM are mostly composite solid propellants, mainly composed of polymer binder matrix, oxidizer, metal particles and other functional additives, etc. There are two phases, the continuous phase composed of the binder matrix and the dispersed phase composed of solid particles such as inorganic oxidizer and metal additives, so the propellants have the mechanical properties of highly filled solid

ISSN: 2414-1895 DOI: 10.6919/ICJE.202301_9(1).0002

composites [2]. One of the static viscoelastic qualities of propellants is creep, which is an important factor influencing material failure. For polymers, creep is present at low stress levels and at room temperature due to the nature of the constituent molecular chains of the polymer and its mobility as well. In order to protect engines from environmental factors during vertical storage, industry usually sets storage conditions at ambient temperature and constant humidity. Even so, the propellant will produce creep effects due to its own weight, and the NEPE propellant has a greater elongation and its creep phenomenon is more severe. The continuous sinking deformation of the pillar is transferred to the bonding interface, which is subjected to load, and the long-term load leads to the creep effect of the interface structure, so the damage of the bonding interface under vertical storage is inevitable, and the stress state needs to be obtained urgently.

The material mechanical properties of SRMs in long-term storage will change with storage time, so the influence of load history of the engine during storage should be considered. Lei et al [3] analyzed the sinking phenomenon of the pillar under vertical storage of foreign large solid rocket engines and illustrated its effect on the bonding interface. On the simulation analysis of vertical storage of the whole SRM, Yuan et al [4] carried out the finite element calculation analysis under vertical storage of a large solid rocket motor and compared the effect of the combustion chamber with and without pressure filling, but only the pillar was analyzed. Wang et al [5] analyzed the stress-strain changes of the pillar and the bonding structure under vertical long-term storage, and the numerical simulation concluded that the maximum stress of the bonding structure after long-time vertical storage was located at the root of the former stress release, reaching 0.6 MPa. However, the analysis of the above researchers mostly focused on HTPB propellant and did not involve NEPE propellant. In this paper, we do not consider the effect of charge aging under SRM vertical storage, but consider the load of engine experiencing curing cooling before vertical storage, which is a factor that must be considered in the analysis of vertical storage. From the characteristics of the combustion chamber structure under curing cooling load and the published domestic and international literature [6-9], it is known that under curing cooling conditions, the bonding interface will generate residual stresses due to the effect of inhomogeneous temperature field, and the thermal stresses and thermal strains caused by the difference in thermal expansion of the interface materials are important causes of subsequent damage. Among the SRM bonding interface failure modes, the most common is debonding at interface III (propellant/liner interface). Therefore, this section uses ABAQUS finite element software to analyze the stresses and strains at the III interface under curing and cooling and vertical storage.

2. Finite Element Model

2.1 Physical Model and Meshing

A NEPE propellant engine combustion chamber as the object of study, the engine diameter of about 2 meters, length of about 4 meters, for the charge using wall pouring type, the combustion chamber using the wing column type charge structure, the front of the pillar for the umbrella disk structure, evenly distributed 8 wing grooves, the pillar in the middle for the cylindrical section of the tube type charge, the pillar tail section for the same 8 wing grooves evenly distributed umbrella disk type structure, insulation layer in the engine pillar and shell contact arc parts at Set stress release. Due to the small thickness of the liner material, it is merged with the insulation in the modeling as well as the mesh drawing. Referring to the settings of the literature [10-12] and so on, only the insulation is set in the SRM whole engine simulation calculation without the liner layer, but in order to study the bonding characteristics of the liner layer and the propellant interface, the liner material properties are assigned to the insulation in the model. According to the symmetry of combustion chamber structure, take 1/16 engine combustion chamber entity for 1:1 3D modeling, draw the plane sketch of 1/2 engine axial section in CAD software, then import the .dxf file into ABAQUS to establish the 3D rotating solid model, after cutting to present the wing slot on the pillar, and carry out the subsequent simulation calculation after the modeling is completed, the specific structure is shown in Figure 1

ISSN: 2414-1895 DOI: 10.6919/ICJE.202301_9(1).0002

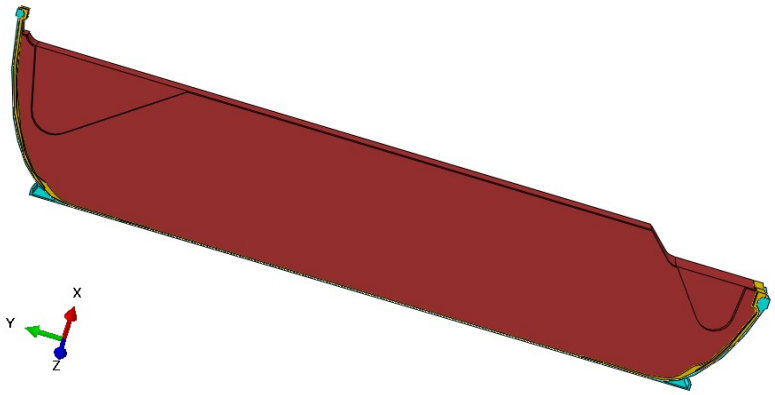

Figure 1. 1/16 SRM model structure schematic

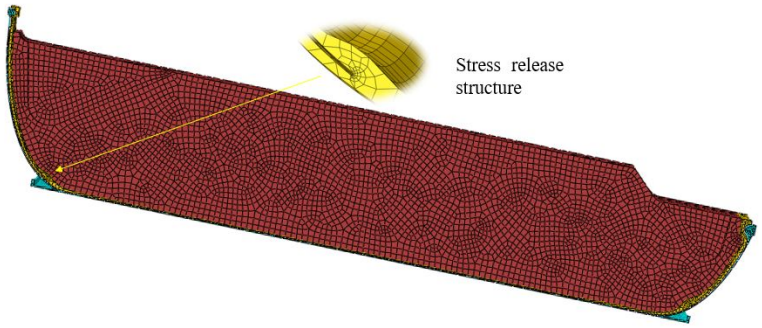

Figure 2. 1/16 SRM model meshing

For the engine charge structure, a structured hexahedral mesh is adopted, and the cell type is C3D8, a three-dimensional eight-node solid cell, with a total of 55,552 cells and 73,243 nodes, as shown in Figure 2.

2.2 Material Parameters

The parameters of the shell, insulation (liner) and propellant material in this section are shown in Table 1. The propellant pillar is a viscoelastic material, and the longer the load action time, the closer the mechanical properties of the viscoelastic material are to the equilibrium state, and the elastic solution expressed by the equilibrium modulus is close to the viscoelastic solution [12,13]. In order to simplify the calculation, the elastic solution is used in ABAQUS for the calculation, and the same method is used for the insulation (liner), and the material parameters are set with reference to the literature [11].

Table 1. Material parameters of SRM parts

Material parameter	Propellant pillar	Insulation (liner)	Shell
Density /(kg/m^3)	1840	1200	7800
Coefficient of expansion /K^{-1}	1.3e^{-4}	1.2e^{-4}	1.1e^{-5}
Poisson ratio	0.499	0.495	0.3
Young's modulus /MPa	0.6	1.2	210000

2.3 Calculation and Boundary Conditions

2.3.1 Calculation of Working Conditions

The residual stress after curing and cooling down of the pillar has been present in the whole engine service process, which has an important influence on the simulation calculation of the pillar under gravity load and cannot be ignored. The temperature field in the curing and cooling slowly cools naturally from the initial zero stress temperature of 58°C to room temperature of 20°C. When the

ISSN: 2414-1895 DOI: 10.6919/ICJE.202301_9(1).0002

curing and cooling process is completed after 4 days, the temperature inside the pillar basically equilibrates. The vertical storage process first considers the combustion chamber subjected to transient gravitational loads, and then the long-term effect of gravitational loads leads to creep of the pillar, which affects the interface.

2.3.2 Analysis Steps and Boundary Conditions

The analysis step is divided into three steps, the first analysis step is set to the change of prestressing temperature field, and the duration is 345600s, i.e. 4 days. The second analysis step is to apply an acceleration load of 1g, and the third analysis step is to perform creep calculations for 15552000s, i.e. 180 days. The first and third analysis steps are set as viscous analysis steps, and the second analysis step is set as static general analysis step. The outer surface of the shell is restrained by solid support, and the symmetry surface of the whole model is restrained by the corresponding symmetry, the inner surface of the shell and the outer surface of the insulation are in bound contact, the surface of the inner hole of the pillar is the free surface, and the inner surface of the shell is the master surface and the outer surface of the insulation is the slave surface due to the large stiffness of the shell, so the contact between the shell and the insulation is the master surface. The inner surface of the insulation and the outer surface of the pillar also use binding contact, the inner surface of the insulation is the main surface, the outer surface of the pillar is the slave surface.

3. Analysis of Stress State of Bonding Interface

3.1 Mechanical Response of the Bonded Structure

In this paper, the mechanical response of the bonding interface under long-term storage is studied, so the stress state of the pillar is not considered, and the maximum stress on the insulation (liner) of the bonding structure is calculated numerically by ABAQUS. As can be seen from Figure 3, the stress release releases the internal stress between the insulation (liner) and the pillar due to environmental and load factors, reducing the stress level at the interface, but the larger stress concentration may cause it to crack from the root, and the crack will be very dangerous once it expands along the interface between the internal insulation and the pillar. It can be seen that the stress of the bonded structure under long-term storage should not be ignored, especially the stress condition of the root of the stress release.

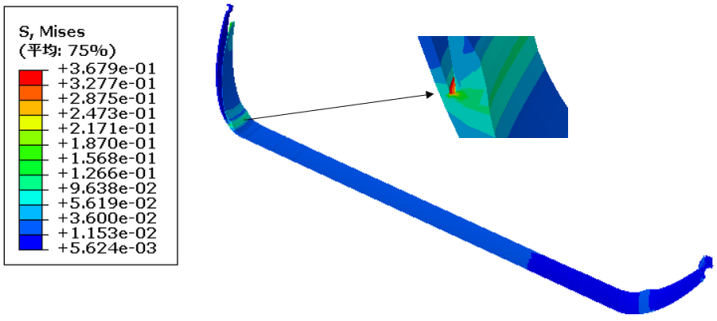

(a) Equivalent stress cloud

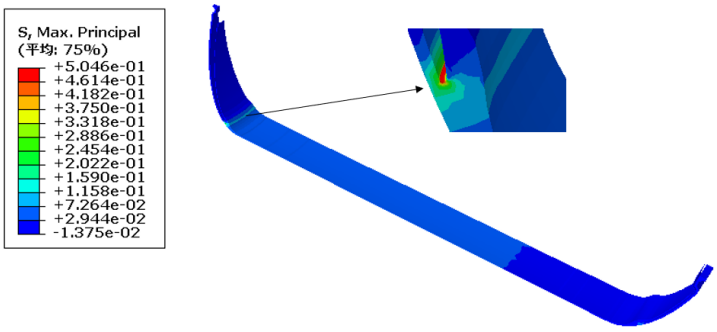

(b) Maximum principal stress cloud

ISSN: 2414-1895 DOI: 10.6919/ICJE.202301_9(1).0002

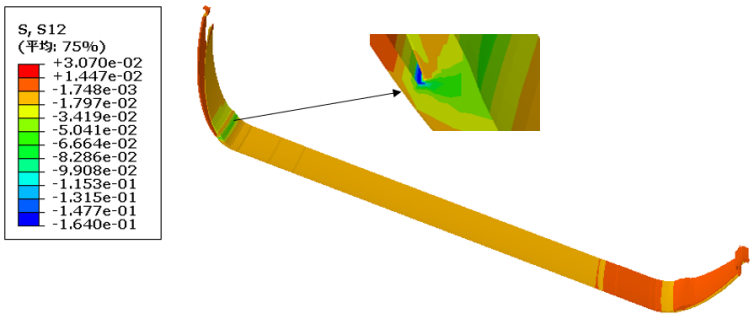

(c) Shear stress cloud

Figure 3. Mechanical response stress cloud of bonded structure

3.2 Analysis of the Distribution Law of the Mechanical Response along the Path

Through numerical simulation analysis, it is found that at the propellant/liner interface, the mechanical response volume along the annular direction does not change significantly and the stress value is small. Therefore, the path shown in Fig. 4 can be selected as a typical path of the engine interface and used to analyze the variation law of stress along the path under long-term storage.

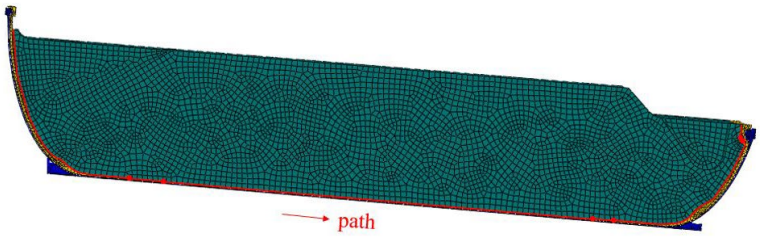

Figure 4. Path selection schematic

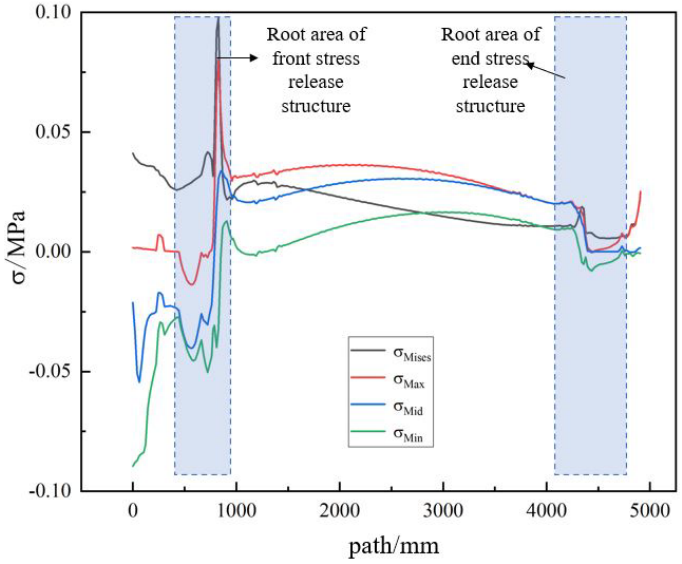

Figure 5. Interfacial equivalent stress along the path

Figure 5 shows the variation of Mises equivalent force, first principal stress, second principal stress and third principal stress along the path of the engine interface under long-term storage. It can be seen from the figure that the stresses change abruptly at the interface near the root of the front stress release, where the Mises equivalent force and the first principal stress are the largest, 0.0978 MPa and 0.0807 MPa, respectively. the stresses are distributed more uniformly in the middle section of the cylinder, where the first principal stress is the largest, 0.0363 MPa. the stresses also change abruptly at the interface near the root of the rear stress release, but their effects can be neglected. The stress value is

ISSN: 2414-1895 DOI: 10.6919/ICJE.202301_9(1).0002

small and its effect can be ignored. In the front area of the insulation, the stress is higher because of the stress concentration at the free end of the stress release, but the stress strain is transferred to the root area of the stress release.

3.3 Three-directional Stress State Analysis

Based on the simulation results, the relationship between the three-way positive stresses σ_{11}, σ_{22}, σ_{33} and the axial shear stress σ_{12} on the interface position is obtained as shown in Figure 6. The positive stresses σ_{11}, σ_{22}, σ_{33} and the axial shear stress σ_{12} are all less than 0 in the front end area, which means that the interface is in a state of three-way compression and shear in this area; in the root area of the stress release, the positive stresses are all greater than zero, with the maximum σ_{22} being 0.0469 MPa and the positive stresses in the other two directions being smaller, and the shear stress σ_{12} is less than zero and has a larger value of -0.0499 MPa, which means that the interface is in a state of three-way tension plus shear in this area. is in a three-way tension plus shear state. Similarly, the interface at the middle section of the barrel is still in a three-way tension plus shear state; at the rear end, it is roughly in a unidirectional tension state. At the propellant/liner interface, the stress value is the largest near the root of the former stress release, which is subjected to shear stress parallel to the interface and tensile stress perpendicular to the interface and can be regarded as the interface subjected to tensile-shear stress.

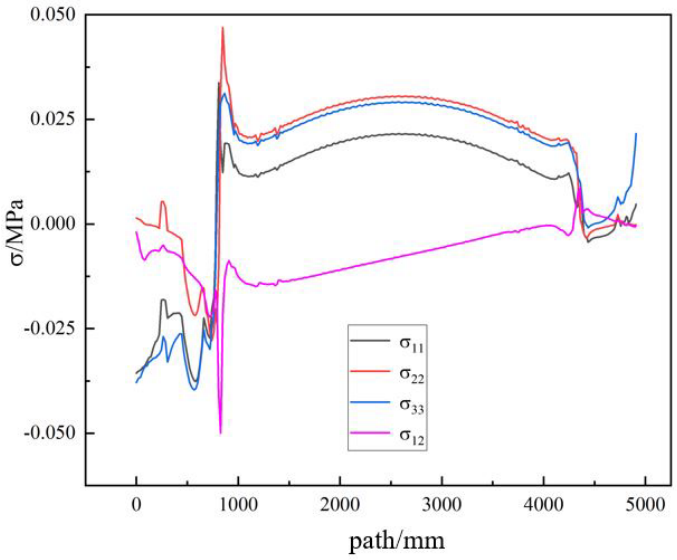

Figure 6. Three-way stress along the path at the interface

4. Conclusion

The stress response of the bonding interface under curing and cooling and vertical storage conditions for 180 days was calculated using the equivalent viscoelastic ontology expressed as the equilibrium modulus of the propellant. The following conclusions were drawn.

(1) Under vertical storage, the danger point of the bonding structure mainly exists at the root of the stress release of the insulation layer, the stress value at the root of the stress release is large and the stress state is complicated, so it is worth studying to prevent the stress release from fracturing at the root and then expanding along the interface.

(2) The stress values at the interface ring upward do not vary significantly, and the stress values on the path from the front end to the back end vary greatly. An abrupt change occurs at the interface near the root of the former stress release, where the Mises equivalent stress is 0.0978 MPa and the maximum principal stress is 0.0807 MPa.

(3) The stress state of the interface is relatively complex, and the propellant/liner interface is in a three-way tensile plus shear state near the artificial debonding root and in the middle section of the

ISSN: 2414-1895 DOI: 10.6919/ICJE.202301_9(1).0002

barrel, and the interface near the artificial debonding root is subject to less stress in two directions, which can be regarded as a mixed tensile and shear stress at the interface.

Acknowledgments

The authors gratefully acknowledge the financial support of the National Natural Funds in China (No. 11772352 and No. 22205259), the Science project of Shaanxi Province (No. 20190504 and No. 2020JQ-486), and Key scientific research projects of colleges and universities in Henan Province (No. 23A590004).

References

[1] X. Wang, M. Gao, P. Wu, et al. Research on creep effect of solid propellant grain under vertical storage, Chinese Journal of Explosives & Propellants, Vol. 42 (2019) No. 2, p. 160-168.

[2] L.F. Hou: Composite solid propellant (Astronautic Press, China 1994), p.327-328. (In Chinese)

[3] N. Lei, X.Y. Yan. Research on aging of large solid rocket motor under vertical storage condition, Journal of Solid Rocket Technology, Vol. 42 (2019) No. 3, p. 419-426.

[4] J. Yuan, P. Ren, G.R. He. Research on vertical storage of large-scale SRM chamber, Journal of Solid Rocket Technology, Vol. 37 (2014) No. 6, p. 809-813+818.

[5] X. Wang, R.Y. Zhao, K. Wang. Structural finite element analysis of solid motor grain under vertical storage, Journal of Ordnance Equipment Engineering, Vol. 41 (2020) No. 8, p. 45-51+102.

[6] Z.C. Zhu, E. Cai. A finite element analysis of three dimensional temperature field and stress fields for solid rocket motor grain, Journal of Propulsion Technology, 1997, No. 2, p. 21-26.

[7] K. Wang, W.P. Tian. Three-dimensional finite-element analysis for fore and aft finocyl grain of solid rocket motor, Journal of Propulsion Technology, 1997, No. 4, p. 36-41.

[8] S.W. Chyuan. A study of loading history effect for thermoviscoelastic solid propellant grains, Computers & Structures, Vol. 77 (2000) No. 6, p. 735-745.

[9] S.W. Chyuan. Nonlinear thermoviscoelastic analysis of solid propellant grains subjected to temperature loading, Finite Elements in Analysis and Design, Vol. 38 (2002) No. 7, p. 613-630.

[10] H.M. Zhou, J.Y. Li, S. Yuan, et al. Temperature field and stress field analysis of SRM's grain during cooling process after curing, Missiles and Space Vehicles, 2015, No. 1, p. 104-106.

[11] Y.Z. Luo. NEPE propellant engine vertical storage suitability analysis and evaluation, Academy of Aerospace Solid Propulsion Technology, 2021.

[12] X.H. Zhang, X.Y. Zheng, H.Y.Li. Stress and strain analysis for solid rocket motor grains with stress-release boot, Chinese Journal of Applied Mechanics, Vol. 29 (2012) No. 4, p. 426-430+487.

[13] R.X. Chen: Solid rocket motor design and research (Astronautic Press, China 1991), p.615-616. (In Chinese)